

High-Conductive Multilayer $\text{TiO}_x\text{-Ti}_3\text{C}_2\text{T}_x$ Electrocatalyst for Longevous Metal-Oxygen Battery under a High Rate

Zhihui Sun, Shuai Zhao *, Jixiong Zhang *

School of Mines, China University of Mining and Technology, Xuzhou 221116, China

* Correspondence: Zhaoshuai6074@cumt.edu.cn (S.Z.); zjxiong@163.com (J.Z.)

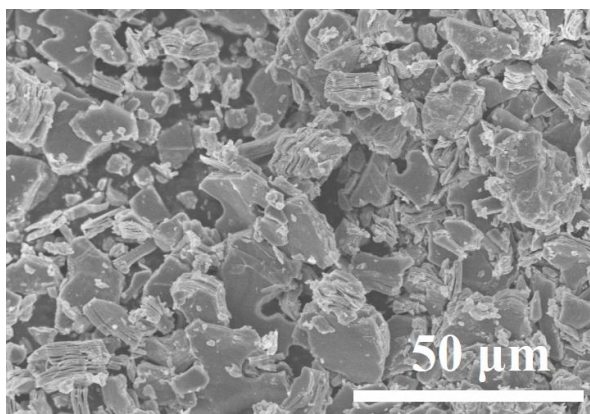


Figure S1. SEM image of $\text{TiO}_x\text{-Ti}_3\text{C}_2\text{T}_x$.

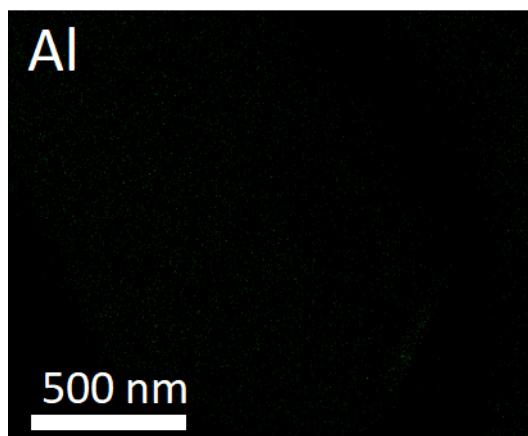


Figure S2. EDS mapping images of Al element for $\text{TiO}_x\text{-Ti}_3\text{C}_2\text{T}_x$.

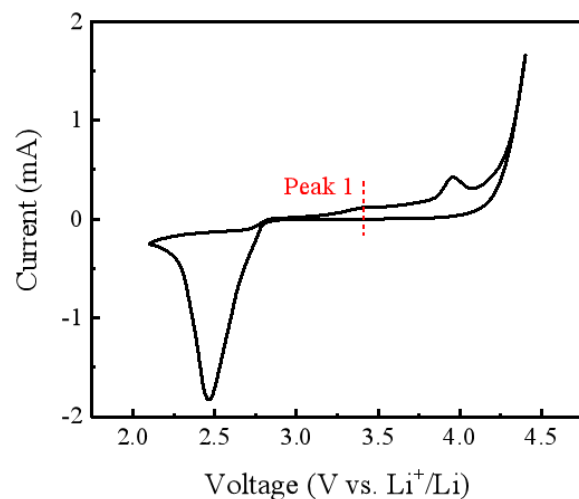


Figure S3. cyclic voltammetry (CV) curves of $\text{TiO}_x@ \text{Ti}_3\text{C}_2\text{T}_x$.

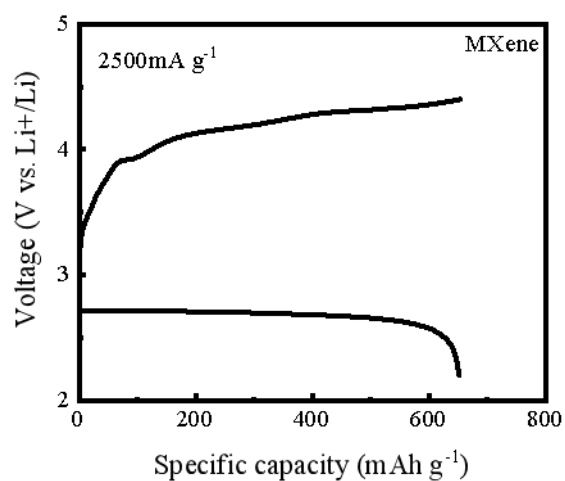


Figure S4. Initial full discharge/charge curves of $\text{TiO}_x\text{-Ti}_3\text{C}_2\text{T}_x$ based LOBs at 2500 mA g^{-1} (The specific capacities are normalized by the weight of actual whole electrodes).

Table S1. EDS elemental analysis of TiO_x-Ti₃C₂T_x.

Element	Weight %	Atomic %	Net Error%□C K
C	19.52	42.13	0.85
O	12.61	20.20	1.72
Al	1.04	0.98	3.98
Ti	67.83	36.69	0.57

Table S2. Comparison of battery performance of TiO_x-Ti₃C₂T_x based electrode with other reported electrodes.

Material	Current density	First discharge capacity	Cycling current density	Cycle number	Limited capacity	Rf.
V-TiO ₂ /Ti ₃ C ₂ T _x	100 mA g ⁻¹	11 487 mAh g ⁻¹	100 mA g ⁻¹	200	1000 mAh g ⁻¹	[1]
N-TiO ₂ /Ti ₃ C ₂ T _x	100 mA g ⁻¹	10122 mAh g ⁻¹	500 mA g ⁻¹	200	500 mAh g ⁻¹	[2]
MoO ₂ /Mo ₂ C@RGO	100 mA g ⁻¹	2365 mAh g ⁻¹	200 mA g ⁻¹	100	1000 mAh g ⁻¹	[3]
MoO ₂ NPs/CTs	0.2 mA cm ⁻²	9.3 mAh cm ⁻²	0.2 mA cm ⁻²	240	0.4 mA cm ⁻²	[4]
MnCo ₂ O ₄ /MoO ₂ @Ni	200 mA g ⁻¹	4210 mAh g ⁻¹	500 mA g ⁻¹	400	1000 mAh g ⁻¹	[5]
TiO _x -Ti ₃ C ₂ T _x	2500 mA g ⁻¹	7169 mAh g ⁻¹	2500 mA g ⁻¹	100	1000 mAh g ⁻¹	

References

- [1] Zheng R., Shu C., Hou Z., Hu A., Hei P., Yang T., Li J., Liang R., Long J., In Situ Fabricating Oxygen Vacancy-Rich TiO₂ Nanoparticles via Utilizing Thermodynamically Metastable Ti Atoms on Ti₃C₂T_x MXene Nanosheet Surface To Boost Electrocatalytic Activity for High-Performance Li–O₂ Batteries, *ACS Appl. Mater. Interfaces*, **2019**, 11, 50, 46696–46704. <https://doi.org/10.1021/acsami.9b14783>
- [2] Zheng X., Yuan M., Guo D., Wen C., Li X., Huang X., Li H., Sun G., Theoretical

Design and Structural Modulation of a Surface-Functionalized $\text{Ti}_3\text{C}_2\text{T}_x$ MXene-Based Heterojunction Electrocatalyst for a Li–Oxygen Battery, *ACS Nano*, **2022**, 16, 3, 4487–4499. <https://doi.org/10.1021/acsnano.1c10890>

- [3] Lu Y., Ang H., Yan Q., Fong E., Bioinspired Synthesis of Hierarchically Porous $\text{MoO}_2/\text{Mo}_2\text{C}$ Nanocrystal Decorated N-Doped Carbon Foam for Lithium–Oxygen Batteries, *Chem. Mater.*, **2016**, 28, 5743-5752. <https://doi.org/10.1021/acs.chemmater.6b01966>
- [4] Liu J., Li D., Wang Y., Zhang S., Kang Z., Xie H., Sun L., MoO_2 nanoparticles/carbon textiles cathode for high performance flexible Li- O_2 battery, *J. Energy Chem.*, **2020**, 47, 66-71. <https://doi.org/10.1016/j.jechem.2019.12.001>
- [5] Cao X., Sun Z., Zheng X., Jin C., Tian J., Li X., Yang R., $\text{MnCo}_2\text{O}_4/\text{MoO}_2$ Nanosheets Grown on Ni foam as Carbon- and Binder-Free Cathode for Lithium–Oxygen Batteries, *ChemSusChem*, **2018**, 11, 574-579. <https://doi.org/10.1002/cssc.201702240>